Atmos. Chem. Phys., 9, 3799–3813, 2009
www.atmos-chem-phys.net/9/3799/2009/

Atmospheric Chemistry and Physics

SCIAMACHY CO over land and oceans: 2003–2007 interannual variability

A. M. S. Gloudemans[1], **A. T. J. de Laat**[1,2], **H. Schrijver**[1], **I. Aben**[1], **J. F. Meirink**[2], **and G. R. van der Werf**[3]

[1]SRON Netherlands Institute for Space Research, Utrecht, The Netherlands
[2]Royal Netherlands Meteorological Institute (KNMI), de Bilt, The Netherlands
[3]Faculty of Earth and Life Sciences, VU University, Amsterdam, The Netherlands

Received: 24 December 2008 – Published in Atmos. Chem. Phys. Discuss.: 2 March 2009
Revised: 23 May 2009 – Accepted: 27 May 2009 – Published: 11 June 2009

Abstract. We present a new method to obtain accurate SCIAMACHY CO columns over clouded ocean scenes. Based on an improved version of the Iterative Maximum Likelihood Method (IMLM) retrieval algorithm, we now have retrieved five years of data over both land and clouded ocean scenes between 2003 and 2007. The ocean-cloud method uses the CH_4 columns retrieved simultaneously with the CO columns to determine the cloud top height. The CH_4 cloud top height is in good agreement with the FRESCO+ cloud top height determined from UV-VIS oxygen-A band measurements, providing confidence that the CH_4 cloud top height is a good diagnostic of the cloud top height over (partially) clouded ocean scenes. The CO measurements over clouded ocean scenes have been compared with collocated modeled CO columns over the same clouds and agree well. Using clouded ocean scenes quadruples the number of useful CO measurements compared to land-only measurements.

The five-year CO data set over land and clouded ocean scenes presented here is based on an improved version of the IMLM algorithm which includes a more accurate determination of the random instrument-noise error for CO. This leads to a smaller spread in the differences between single CO measurements and the corresponding model values. The new version, IMLM version 7.4, also uses updated spectroscopic parameters for H_2O and CH_4 but this has only a minor impact on the retrieved CO columns. The five-year data set shows significant interannual variability over land and over clouded ocean scenes. Three examples are highlighted: the Asian outflow of pollution over the northern Pacific, the biomass-burning outflow over the Indian Ocean originating from Indonesia, and biomass burning in Brazil. In general there is good agreement between observed and modeled seasonal cycles and interannual variability.

Correspondence to:
A. M. S. Gloudemans
(a.gloudemans@sron.nl)

1 Introduction

Carbon monoxide (CO) is an important pollutant and the major sink of OH. Its life time of typically weeks to months (Cicerone, 1988) makes CO a suitable tracer for long range atmospheric transport and consequently the global distribution of air pollution (e.g. Shindell et al., 2006). Long-term global data sets of CO as measured with satellite instruments such as MOPITT (Measurements Of Pollutants In The Troposphere; Deeter et al., 2003) launched in 1999, AIRS (Atmospheric InfraRed Sounder; McMillan et al., 2005) launched in 2002, and SCIAMACHY (SCanning Imaging Absorption spectroMeter for Atmospheric CartograpHY; Bovensmann et al., 1999) launched in 2002 provide good insight in the global changes and interannual variability in air pollution. Significant interannual variability in CO has been reported both near emission sources and over areas affected by long-range transport of pollution (e.g. Edwards et al., 2004, 2006b; Gloudemans et al., 2006; Yurganov et al., 2008). These variations are mostly due to variations in biomass burning which is one of the major sources of CO.

Satellite measurements from MOPITT and AIRS show significant enhancements of CO in the free troposphere over the oceans due to long-range transport (e.g. Heald et al., 2004; McMillan et al., 2005; Bowman, 2006; Edwards et al., 2006a). Our previous SCIAMACHY studies presented only CO measurements over land (de Laat et al., 2006, 2007;

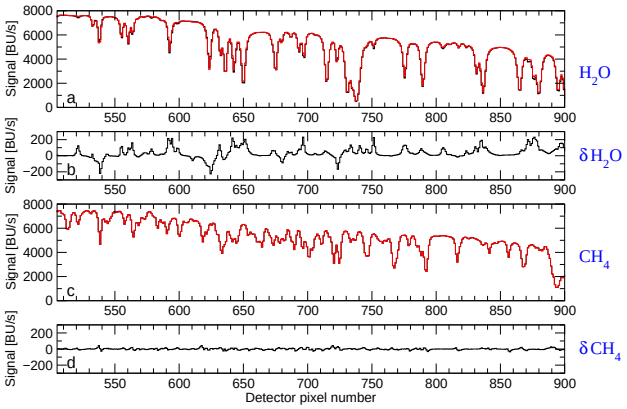

Fig. 1. Differences between HITRAN 2004 and the new spectroscopy used in this paper (see text). The spectra have been simulated using the same forward model as in the IMLM retrieval method which includes both an atmospheric and instrument model converting the reflectance spectra to the measured detector signal in BU/s at SCIAMACHY spectral resolution. The retrieval window used for CO retrievals lies between detector pixel 505 and 615 corresponding to the wavelength range 2324.5–2337.9 nm. **(a)** Simulated atmospheric reflectance spectra of the H_2O lines using the HITRAN 2004 database (black) and the new database from Jenouvrier et al. (2007) (red). **(b)** Difference between the red and black curves from panel (a). **(c)** Simulated atmospheric reflectance spectra of the CH_4 lines using the HITRAN 2004 database (black) and the new database from Predoi-Cross et al. (2006) (red). **(d)** Difference between the red and black curves from panel (c).

Gloudemans et al., 2006). However, a number of publications indicate that ocean observations over clouds still contain valuable information about CO (Frankenberg et al., 2005; Buchwitz et al., 2006, 2007). While the surface reflectance over the oceans in the near-infrared is insufficient to accurately measure CO over cloud-free scenes, the reflectance of clouds is sufficiently high in the near-infrared to obtain accurate CO columns. This allows studying long-range transport of CO over the oceans, since most of the long-range transport of CO takes place above the boundary layer (e.g. Stohl et al., 2002).

Here, a new method is presented to study SCIAMACHY CO over (partially) clouded ocean scenes over boundary layer clouds by using the simultaneously retrieved methane column (CH_4) to estimate the cloud top height. Together with a five-year data set of SCIAMACHY CO observations covering the period 2003–2007 this allows to study the interannual variability of CO on a global scale. This paper is organized as follows: Sect. 2 describes the new retrieval version, the TM4 model, and statistical analysis of the new CO data set. Section 3 presents the new method to obtain accurate CO columns over clouded ocean scenes. Section 4 presents three examples of interannual variability seen in the SCIAMACHY CO measurements and the conclusions are presented in Sect. 5.

2 CO column data

2.1 SCIAMACHY CO total columns

The SCIAMACHY CO total columns presented here have been retrieved with the Iterative Maximum Likelihood Method (IMLM) algorithm in the near infrared wavelength range between 2324.5–2337.9 nm (Schrijver, 1999; Gloudemans et al., 2005, 2008). This spectral region is sensitive to the whole column, with almost uniform sensitivity from ∼200 hPa down to the surface (Gloudemans et al., 2008). The most recent version of the retrieval algorithm, version 7.4, is used here. This version differs from version 6.3 used previously (de Laat et al., 2006, 2007; Gloudemans et al., 2006, 2008). The main difference is that the contribution of detector noise to the random instrument-noise error of a single CO measurement is estimated using the corresponding in-flight dark current measurements per individual detector pixel instead of assuming an average value for the detector-noise contribution over the whole spectral range based on pre-flight measurements as done in version 6.3 (cf. Eq. (7) in Gloudemans et al. (2008) for details on the calculation of the instrument-noise error). This results in a more accurate determination of the instrument-noise error for every single CO measurement.

Another important difference is that in IMLM version 7.4 the self-broadening of the H_2O lines is included in the calculation of the cross-sections contrary to version 6.3 where this was neglected, and updated cross-sections for H_2O and CH_4 are used. Version 7.4 includes the spectral data base for H_2O from Jenouvrier et al. (2007) for the calculation of the cross sections and line broadening instead of the HITRAN2004 database (Rothman et al., 2005) used in version 6.3.

The top two panels of Fig. 1 show the difference between these two databases in the 2.3 μm spectral region using simulated atmospheric reflectance spectra for H_2O at the SCIAMACHY spectral resolution. The CO retrievals are performed between detector pixel 505 and 615 corresponding to the wavelength range 2324.5–2337.9 nm. The two databases show significant differences in this spectral range. For CH_4 the HITRAN2004 broadening coefficients have been replaced with those published by Predoi-Cross et al. (2006) but the differences between these two databases are much smaller than the differences for H_2O as can be seen in the bottom two panels of Fig. 1.

Figure 1 demonstrates that there can be significant differences between different spectroscopic databases. However, in the case of SCIAMACHY CO, comparison of CO results obtained with the HITRAN 2004 data base with those obtained with the updated spectroscopic parameters for H_2O and CH_4 shows only a minor impact on the retrieved CO total columns. This is in agreement with the findings by Gloudemans et al. (2008) who have investigated the effect of spectroscopic errors in H_2O and CH_4 on the retrieved CO total columns using simulated spectra. On the other hand,

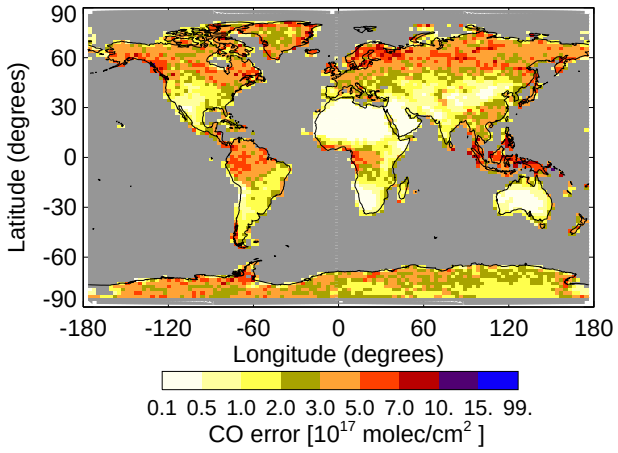

Fig. 2. Global distribution of the average SCIAMACHY CO monthly-mean instrument-noise error in 2004 on a 3° by 2° grid for IMLM version 7.4. Blue indicates large instrument-noise errors, white indicates small instrument-noise errors.

the H_2O total columns which are retrieved simultaneously with the CO total columns from the 2.3 μm SCIAMACHY spectra show an improved correlation with the ECMWF H_2O columns compared to those of IMLM version 6.3 (cf. Gloudemans et al., 2008). Although the updated H_2O and CH_4 spectroscopic parameters have only a minor effect on the retrieved CO total columns between 2324.5–2337.9 nm used in this paper, accurate spectroscopic parameters are nevertheless important for the retrieval of trace gases in the 2.3 μm wavelength range.

Figure 2 shows a map of the global distribution of the monthly mean instrument-noise error for IMLM version 7.4. Note that the distribution is similar to what is shown in Gloudemans et al. (2008) but the values are somewhat lower, especially in regions with low surface albedos, such as in South-East Asia. This is due to the more accurate calculation of the instrument-noise error in IMLM version 7.4.

Previous publications used SCIAMACHY CO total columns for shorter periods up to one year (de Laat et al., 2006, 2007; Gloudemans et al., 2006, 2008; Turquety et al., 2008). Here, we present five years of global SCIAMACHY CO column data covering January 2003–December 2007 obtained with IMLM version 7.4. The global distributions of the instrument-noise errors for the years 2003, 2005, 2006, and 2007 are very similar to the 2004 distribution shown in Fig. 2.

2.2 TM4 Model

The SCIAMACHY CO columns in this paper are compared with the CO total columns from the chemistry-transport model TM4 (Meirink et al., 2006). This is the same model as used in Gloudemans et al. (2006) and de Laat et al. (2007) and provides CO columns on a $3^\circ \times 2^\circ$ lon-lat grid. A detailed description of the natural and anthropogenic CO emissions used in the TM4 model can be found in de Laat et al. (2007) and references therein. This model uses the Global Fire Emission Database version 2 (GFEDv2) biomass-burning emissions for the period 2003–2007 which are based on satellite measurements of fire counts and burned area (Giglio et al., 2006) and biogeochemical modeling (van der Werf et al., 2006). The global GFEDv2 CO biomass-burning emissions for 2003, 2004, 2005, 2006, and 2007 are 397, 405, 411, 392, and 410 Tg CO yr^{-1}, respectively (cf. http://www.geo.vu.nl/users/gwerf/GFED/data/readme.pdf).

For comparison with SCIAMACHY observations model results are always sampled for the same day at the SCIAMACHY overpass time of 10:00 a.m. and for the model grid cell corresponding to the geographical location of the individual observations.

2.3 Statistical analysis

The quality of the IMLM v7.4 CO columns has been evaluated by performing a statistical analysis similar to the analysis presented in de Laat et al. (2007). They show that differences between single SCIAMACHY CO measurements and corresponding TM4 model results are primarily explained by the SCIAMACHY random instrument-noise errors and that these are thus a good diagnostic for the precision of the CO total column measurements. The results of the statistical analysis for version 7.4 in comparison with version 6.3 are shown in Fig. 3 using single CO measurements and the corresponding model results for the year 2004. The spread in the differences between single CO measurements and the corresponding model values, expressed as the root-mean-square (rms) of the differences, is smaller for version 7.4 than for version 6.3, except for instrument-noise errors smaller than $\sim 0.1 \times 10^{18}$ molecules/cm^2 where they are comparable. For those errors the spread in the differences is similar to the spread in the corresponding modeled CO total columns.

With a perfect model, the differences between observations and model results should be comparable to the instrument-noise error. However, there exist model inaccuracies – for example the use of monthly mean rather than daily emissions, emission errors, and the spatial resolution of $3^\circ \times 2^\circ$ which is considerably larger than that of the CO measurements – as well as retrieval errors not related to the random instrument noise such as minor calibration errors and aerosols as discussed in Gloudemans et al. (2008). These model inaccuracies cause differences that, below a certain instrument-noise error level, dominate the differences between observations and model results. This may explain why the spread for small instrument-noise errors is similar in both retrieval versions. The smaller rms differences between observed and modeled CO for IMLM version 7.4 are also reflected in the slope of the ordinary linear regression and correlation coefficient of the instrument-noise error vs. the SCIAMACHY-TM4 differences which are 2.19±0.03

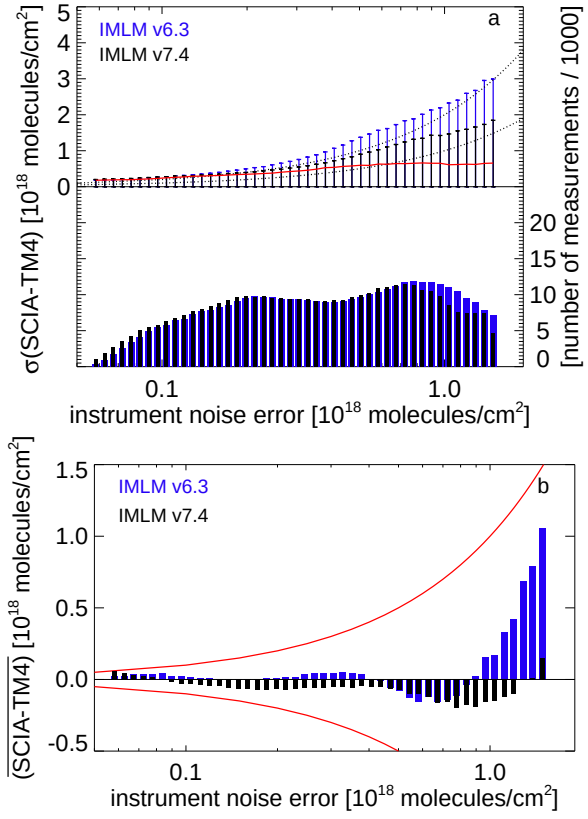

Fig. 3. Comparison of the SCIAMACHY CO total columns from the IMLM retrieval version 6.3 and 7.4 based on single SCIAMACHY measurements over land for the period January to December 2004. **(a)** Root mean square (rms) values of the differences between the single SCIAMACHY CO measurements and the spatially and temporally collocated TM4 CO total columns as function of the instrument noise error. The blue bars indicate the distribution based on IMLM v6.3 retrievals, the black bars based on IMLM v7.4 retrievals. The dotted lines indicate the 1- and 2-σ instrument-noise error levels. The red line indicates the rms value of the TM4 simulated CO total columns, which is caused by spatio-temporal CO total column variations because observations with similar instrument-noise errors can be scattered around the globe. The blue (IMLM v6.3) and black (IMLM v7.4) bars in the bottom panel denote the number of measurements for each instrument-noise interval. **(b)** Average differences between the single SCIAMACHY CO measurements and the spatially and temporally collocated TM4 CO total columns as function of the instrument-noise error. The bars indicate the mean difference for each instrument-noise interval. The blue bars indicate data from the IMLM retrieval version 6.3, the black bars version 7.4. The red line indicates the 1-σ instrument-noise error levels.

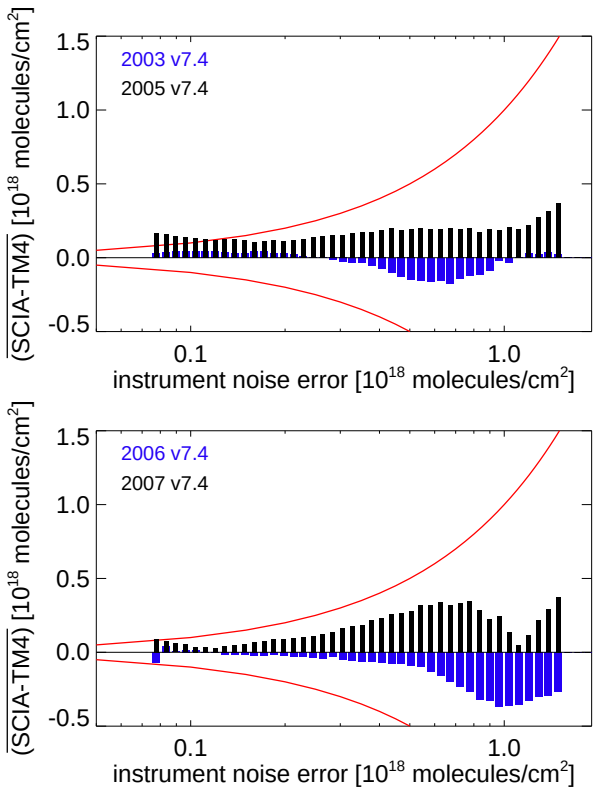

Fig. 4. Average differences between the single SCIAMACHY CO measurements over land and the spatially and temporally collocated TM4 CO total columns as function of the instrument-noise error for different years using the IMLM retrieval version 7.4. The bars indicate the mean difference for each instrument-noise interval. The red line indicates the 1-σ instrument-noise error levels. Top: 2003 (blue) versus 2005 (black). Bottom: 2006 (blue) versus 2007 (black).

and R^2=0.993 for version 6.3, and 1.14±0.01 and R^2=0.994 for version 7.4, respectively.

The bias between single CO measurements and the corresponding model results is similar for both retrieval versions for errors $<1.5\times10^{18}$ molecules/cm^2 and falls within the 1-σ instrument-noise errors (Fig. 3). This confirms that the largest difference between the IMLM version 7.4 and version 6.3 CO total columns is due to the more accurate calculation of the instrument-noise error and only to a minor extent due to the updated spectroscopic parameters (see Sect. 2.1).

In addition to the IMLM version 7.4 statistical analysis for the year 2004 similar analyses have been performed for the years 2003, 2005, 2006, and 2007. The spread in the differences between single CO measurements and the corresponding model values shows a similar behavior as in Fig. 3a for all years. Figure 4 shows that the biases between observed and modeled CO are somewhat different for the other years than for 2004 (cf. Fig. 3b), but well within the 1-σ instrument-noise errors. Some exceptions occurred for very low instrument-noise errors, but these are still within the 2-σ instrument-noise errors (Fig. 4). Part of the variability in the biases for all years may be caused by interannual variations in e.g. the biomass-burning emissions which may be

underestimated in the TM4 model (e.g. Gloudemans et al., 2006) and/or variations in the aerosol loads, thereby overestimating observed CO columns (Gloudemans et al., 2008). The biases shown here denote only the global bias. Locally, the biases may be different, e.g. due to model imperfections or geographically varying retrieval errors such as those due to aerosols.

3 CO observations over low clouds

3.1 Clouds and cloud top height

Previous studies using IMLM CO column observations only show data over land with cloud fraction <0.2 and instrument-noise errors $<1.5\times10^{18}$ molecules/cm^2 (de Laat et al., 2006, 2007; Gloudemans et al., 2006, 2008; Turquety et al., 2008). This selection criterion basically removes all measurements over the oceans, since the sea surface reflectance around 2.3 μm is very low, with typical values of <0.01. For such low reflectances, observations are of insufficient accuracy to be useful. In comparison, the surface reflectance over land typically ranges from 0.05 over densely vegetated areas to more than 0.5 over dry desert regions. However, other studies of SCIAMACHY CO (Frankenberg et al., 2005; Buchwitz et al., 2006, 2007) indicate that ocean observations over clouds still contain valuable information about CO. The presence of CO information over clouds is related to the high reflectance of clouds in the 2.3 μm wavelength range, typically 0.3–0.5 based on completely clouded ground scenes. The cloud reflectance is more than an order of magnitude higher than the sea surface reflectance, implying that for partly clouded scenes the contribution to the retrieved CO column from the cloud-free part of the measurement over the ocean is negligible compared to the clouded part. Thus, if a cloud is detected in the 2.3 μm footprint over the oceans, the CO column retrieved from this measurement represents the CO column above the cloud. This column is independent of the cloud fraction, as long as some cloud is present, which is ensured by using only measurements with cloud fraction >0.2 (cf. Sect. 3.2).

In order to compare these columns with other measurements or model calculations, the cloud top height can be estimated from the CH_4 total columns retrieved from the same spectral window. The cloud top height can then be used to compare the observed CO partial column with a corresponding partial column from a model or another measurement. Another option is to supplement the observed partial column with model values to obtain a total column. Alternatively, the partial column can be converted to a total column by scaling the partial column using the cloud top height. Gloudemans et al. (2008) show that in case of high aerosol loads over land the CO/CH_4 ratio provides more accurate values than the CO total column without correction for aerosols. Buchwitz et al. (2006) scale the CO (partial) column measurements to correct for calibration errors and differences in the light path, e.g. due to aerosols and clouds.

However, the vertical profiles of CO and CH_4 can differ significantly, which is relevant for the scaling method. An analysis based on modeled CO profiles over sea indicates that using the CO/CH_4 column ratio to obtain total columns for CO measurements above clouds causes deviations from the true total columns. Its sign depends on the shape of the CO profile and the CO columns. In the Northern Hemisphere, where boundary layer CO is generally high compared to free tropospheric CO, the method using the CO/CH_4 ratio typically underestimates the true total columns. In the tropics and in the Southern Hemisphere, where free tropospheric CO tends to be higher than boundary layer CO, the method overestimates the true total column. Globally the average differences are $\sim$2.5% for a cloud at 800 hPa, i.e. a boundary layer cloud. However, locally the differences can easily be $>10\%$ and for individual cases even $>50\%$. These differences increase with increasing cloud height: for a 500 hPa cloud, the global differences are on average $\sim$8.5%, but locally they can be $>75\%$. Given the high variability of CO amounts and CO profile shapes, interpretation of CH_4-scaled CO total columns over clouded ocean scenes is complicated.

Therefore, we prefer not to use the CO/CH_4 ratio method. Instead, the partial CO columns above clouded ocean scenes are used together with the corresponding cloud top height for comparison with other satellite data or chemistry transport models, such as the TM4 model used in this paper. The advantage of these partial columns is that they represent the true measurements above the cloud without adding external information which could introduce additional errors. The CH_4 columns, which are retrieved simultaneously with CO from the 2.3 μm measurements, provide a good diagnostic of the cloud top height over clouded ocean measurements. Variations in CH_4 due to cloud top height variations are much larger than spatio-temporal variations in the CH_4 columns, and SCIAMACHY 2.3 μm CH_4 column measurements have almost uniform sensitivity down to the surface as shown by their total column averaging kernels (Gloudemans et al., 2008). Applying the CH_4 averaging kernels to modeled CH_4 profiles has an effect of less than 1% for solar zenith angles $<70°$. For comparison, a 1–2% uncertainty in the CH_4 column would result in a cloud top height uncertainty of 10–20 hPa. Furthermore, Gloudemans et al. (2008) show that the average difference between single CH_4 measurements and the corresponding modeled CH_4 columns for IMLM v6.3 is generally $<5\%$ of the CH_4 total column, even for large instrument-noise errors of up to 1×10^{19} molecules/cm^2 which correspond to about 25% of the CH_4 total column. For IMLM v7.4 similar differences are found. Comparing measured partial CH_4 columns above clouded scenes with corresponding modeled CH_4 total columns can thus be used to estimate the cloud top height over clouded ocean measurements.

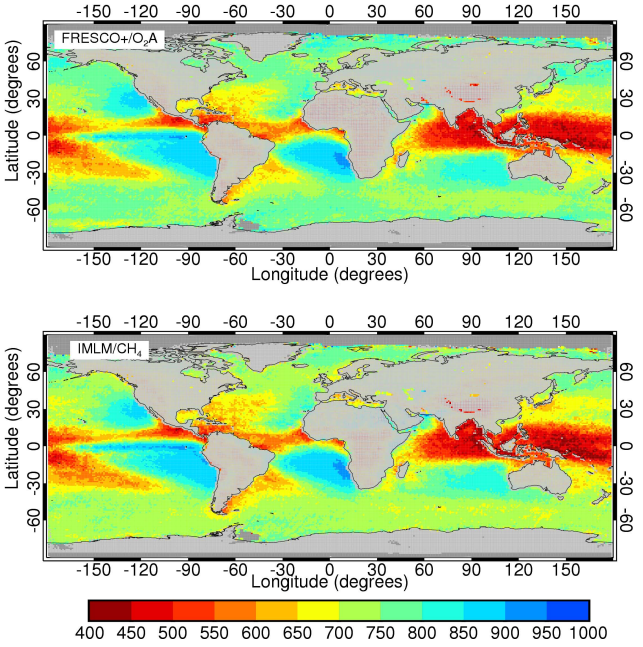

Fig. 5. Global distribution of cloud top height in hPa based on daily gridded $1^\circ \times 1^\circ$ data for the period 2003–2007. Top panel: cloud top height from the FRESCO+ algorithm using the SCIAMACHY O_2-A band. Bottom panel: average cloud top height based on the ratio between the SCIAMACHY IMLM 2.3 μm CH_4 column and TM4 CH_4 column over sea. Only data with a cloud fraction >0.2 as determined by the SPICI algorithm (Krijger et al., 2005) have been included in both panels. Blue indicates low cloud top heights, i.e. high pressures, and red indicates high top cloud heights (low pressures).

Over land, CH_4 is not a good diagnostic of the cloud top height for partially clouded scenes. For partially clouded scenes the cloud albedo is much more comparable to that of the cloud-free part and thus the CH_4 retrieved column represents an average of the cloud-free and clouded part of the measurements. In addition, the CH_4 column of the cloud-free part is influenced by the surface elevation. Partially clouded measurements can thus only be used if the cloud albedo, surface albedo, and cloud fraction are known accurately. For 2.3 μm measurements this is complicated, since the SCIAMACHY spatial resolution is very coarse – 120×30 km – and it is not clear which part of the measurement is clouded while the surface albedo may vary rapidly within one SCIAMACHY ground pixel. For completely clouded land scenes, CH_4 columns might be a good diagnostic of the cloud top height. However, given the large foot print of the 2.3 μm measurements the number of completely clouded measurements is limited and thus does not add a significant amount of data over land compared to what is already used for CO, i.e. data with cloud fraction <0.2 and instrument-noise error $<1.5 \times 10^{18}$ molecules/cm^2. Therefore, partially clouded measurements are only considered over the oceans and not over land.

Figure 5 shows a global map of the cloud top height based on CH_4 columns retrieved simultaneously with the CO columns from the 2.3 μm measurements in comparison with the cloud top height derived from FRESCO+ (Wang et al., 2008). FRESCO+ uses oxygen A-band absorption around 760 nm to estimate cloud top heights. The SCIAMACHY cloud top heights are calculated from the ratio observed over modeled CH_4 total column multiplied with the surface pressure provided by the TM4 model. The observed CH_4 column represents the CH_4 column above the cloud in a $1^\circ \times 1^\circ$ daily grid box while the modeled CH_4 column represents the corresponding true total column. Only CH_4 measurements with a cloud fraction >0.2 have been used. This ensures that at least some cloud is present, since the cloud fraction of the single SCIAMACHY 2.3 μm measurements as provided by the SPICI algorithm (Krijger et al., 2005) mostly provides an upper estimate of the actual cloud cover. Only in exceptional cases where thin wisps of clouds are present the SPICI algorithm may miss these clouds leading to an underestimate of the actual cloud cover. However, using the FRESCO+ cloud fraction instead of the SPICI cloud fraction does not show significantly different results suggesting that this only plays a role for almost cloud-free observations. Using a cloud fraction of >0.2 for clouded measurements is also in agreement with publications by de Laat et al. (2006) and de Laat et al. (2007) who use a cloud fraction of <0.2 to denote measurements with negligible cloud cover.

The cloud top heights from the CH_4 column and FRESCO+ method show very similar spatial variations and reflect some well known patterns (Fig. 5). Areas of persistent subtropical low altitude clouds (stratocumulus) over oceanic upwelling regions can be identified west of southwestern Europe and northern Africa, west of the United States, west of South America, west of southern Africa and west of Australia. Areas of persistent high clouds are found along the equator, as well as the southern Pacific and southern Atlantic convergence zones. Very persistent high clouds occur over Indonesia and over the northern Indian Ocean during the summer monsoon. Note that for many convective equatorial regions there are either persistent high clouds or very few clouds whereas persistent low clouds rarely occur.

It should be noted that the FRESCO+ cloud top height provides the optical mid-level of the cloud (Wang et al., 2008), while the SCIAMACHY cloud top heights based on the CH_4 are representative for the cloud top.

Figure 6 shows the latitudinal agreement between CH_4 cloud top pressures and the FRESCO+ cloud pressures over the oceans for high and low clouds. For low clouds between the surface and 800 hPa the CH_4 and FRESCO+ cloud top heights agree well with an average difference of 17 hPa. For higher clouds with cloud top heights <800 hPa, the agreement is also quite good with an average difference of 14 hPa. These differences are small compared to the $<5\%$ precision of the measured CH_4 columns. Thus the SCIAMACHY 2.3 μm CH_4 columns are a good diagnostic for the cloud

top height of clouded ocean scenes. The average rms values of IMLM-FRESCO+ cloud top height differences – 68 and 86 hPa for low and high altitude clouds, respectively – are much larger than the differences themselves.

3.2 Selection criteria

When SCIAMACHY CO measurements above clouds are compared with models or other satellite data the cloud top height determined from the corresponding CH_4 columns as described in the previous section can be used to ensure a proper comparison. Including CO measurements above clouded ocean scenes almost quadruples the number of useful measurements. A disadvantage of this method is that the part of the CO column below the cloud is missing. However over sea, no major CO sources are present and CO variability is dominated by transport processes and photochemistry.

Transport can take place both in the marine boundary layer as well as in the free troposphere. However, the residence time of pollution (including CO) is generally much longer above the marine boundary layer due to lower temperatures and slower photochemical destruction. Furthermore, wind speeds are generally larger and more zonally oriented in the free troposphere compared to the boundary layer. In addition, at mid-latitudes advection of pollution is often associated with the passage of frontal systems, which tend to transport pollution quickly to higher altitudes. All these factors generally favor free tropospheric intercontinental long range transport.

Therefore, only CO measurements over sea above clouds with cloud top heights between the surface and 800 hPa, i.e. only boundary layer clouds, are considered in order not to miss a significant part of the measured column. This corresponds to measurements over clouded ocean scenes with an associated ratio of observed CH_4 over modeled $CH_4 > 0.8$. As in Sect. 3.1, the observed CH_4 column represents the column above the cloud in a $1^\circ \times 1^\circ$ grid box whereas TM4 provides the corresponding CH_4 total column. In addition, as already noted in Sect. 3.1, only ocean scenes with a cloud fraction >0.2 as determined by the SPICI algorithm are included in order to ensure that at least some cloud is present. A comparison of the cloud fraction with the instrument-noise error indicates that cloudy ocean observations with a cloud fraction of 0.2 or more correspond to CO measurements with instrument-noise errors less than 1.5×10^{18} molecules/cm^2. Figure 7 shows the global distribution of the average monthly CO instrument-noise error in 2004 on a 3° by 2° grid for IMLM version 7.4 over land and sea. The data over land are the same as in Fig. 2. Over the oceans, especially in regions with persistent high clouds (cf. Fig. 5) the noise error is largest. In these regions few boundary layer clouds are present, mostly with a relatively low cloud fraction per individual measurement, resulting in a lower measured signal and thus a larger instrument-noise error (de Laat et al., 2007). On the other hand, regions with persistent subtropical low altitude clouds over oceanic upwelling regions (see Sect. 3.1) have the smallest errors of all ocean scenes. These regions are characterized by extensive continuous boundary layer clouds resulting in a large cloud fraction per measurement and thus a larger signal and a smaller instrument-noise error. The fact that these clouds are present most of the time also results in a large number of clouded measurements which further reduces the monthly-mean instrument-noise error.

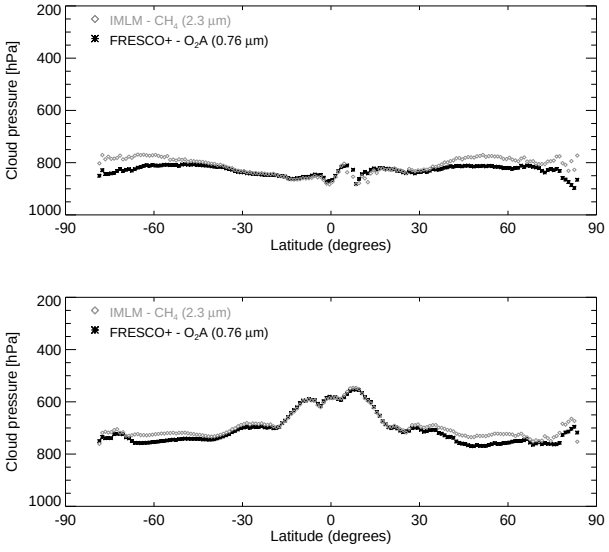

Fig. 6. Latitudinal variation of IMLM CH_4 cloud top pressures (grey) and the FRESCO+ cloud pressures (black) over the oceans in hPa for high and low clouds using the same data as in Fig. 5. Top panel: low clouds with cloud top heights between the surface and 800 hPa. The bias between FRESCO+ and IMLM CH_4 is 17 hPa and the correlation R^2 is 0.69. Bottom panel: high clouds with cloud top heights <800 hPa. The bias between FRESCO+ and IMLM CH_4 is 14 hPa and the correlation R^2=0.98.

Figure 8 shows the statistical analysis of the single CO measurements over clouded ocean scenes for the period January to December 2004 in comparison to those over land which have already been shown in Fig. 3. Over land only CO measurements satisfying the selection criteria used in de Laat et al. (2006, 2007), i.e. a cloud fraction of <0.2 and instrument-noise error $<1.5\times10^{18}$ molecules/cm^2, are used. The spread in the differences between observed and modeled CO is very similar for measurements over land and over clouded ocean scenes. Note that the total number of observations over clouded ocean scenes is $\sim$2.5 times larger than the land-only measurements. The average difference between observed and modeled CO is also similar for instrument-noise errors less than 1×10^{18} molecules/cm^2. This confirms that the CH_4 cloud top height is accurate enough not to have a significant impact on the comparison of the CO partial columns above clouded ocean scenes with other data sets nor on the CO total columns over the oceans after filling-up

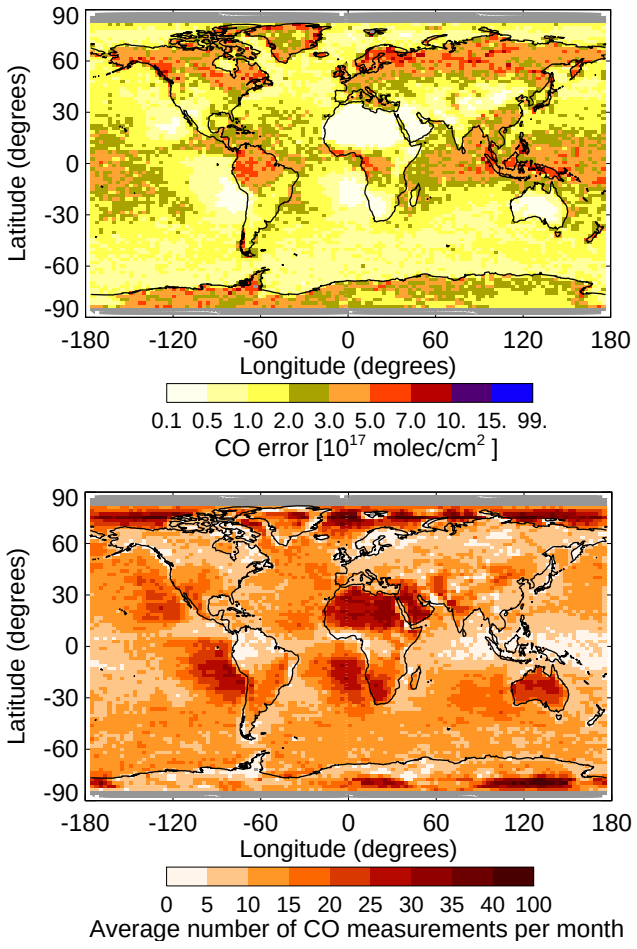

Fig. 7. Top panel: global distribution of the average SCIAMACHY CO monthly-mean instrument-noise error in 2004 on a 3° by 2° grid for IMLM version 7.4 over land and sea. Blue indicates large instrument-noise errors, white indicates small instrument-noise errors. The data over land are the same as in Fig. 2. Bottom panel: geographical distribution of the average number of CO measurements per month based on the same data as in the top panel.

the column below the cloud. For larger instrument-noise errors the clouded ocean observations have a larger average difference than the land-only measurements. Some of these have an average difference significantly larger than the 1-σ instrument-noise error level, but these are still within the 2-σ instrument-noise error level. It should be noted that this concerns less than ∼4000 of the more than 900 000 clouded ocean measurements. Part of these differences could be related to an underestimation of emissions in the TM4 model resulting in less CO transport over the oceans. Especially over Asia, the TM4 emissions are known to be too low (cf. Sect. 3.3), underestimating CO transport over the northern Pacific where the instrument-noise errors are typically $>1\times10^{18}$ molecules/cm^2 (Fig. 7). The years 2003, 2005, 2006, and 2007 show similar statistics as 2004 and are therefore not shown separately. The availability of CO measurements over the oceans in addition to those over land leads to an average total of 1 200 000 CO measurements per year which can be used in inverse modelling studies and/or data assimilation.

The probability distributions of the CO measurements over land and over clouded ocean scenes for 2004 are shown in Fig. 9. The distributions over land and over sea are in good agreement with the corresponding distribution of modeled columns when the model values are convoluted with random noise corresponding to two times the mean instrument-noise error. Without this convolution the distribution of modeled columns is much narrower as the model does not provide estimates of its uncertainties.

3.3 CO Results over the oceans

Figure 10 shows the annual mean measured and modeled CO columns above low clouds over the oceans on a 1° by 1° grid for the years 2003–2007. Only grid boxes with more than 10 CO measurements per year are included. Here the modeled CO columns also only represent the column above the cloud using the CH_4 cloud top height as described in Sect. 3.1. Generally there is good agreement between observed and modeled CO above clouded ocean scenes, but differences are also visible. Outflow regions over the equatorial Atlantic Ocean and the northern Pacific can be discerned in both data sets, but the observed CO columns tend to be higher than the corresponding model values. This is probably caused by too low emissions in the model (Shindell et al., 2006). The gradient between the clean Southern Hemisphere and the polluted Northern Hemisphere is clearly visible in both observed and modeled CO above clouded ocean scenes, although the observed CO seems to be lower than modeled CO at high southern latitudes. This could be due to some remaining calibration errors in the CO measurements (cf. Gloudemans et al., 2008) which have the largest effect in regions with low signal levels and low CO columns which typically occur at high southern latitudes.

Figure 11 shows a five year average of measured and modeled CO total columns on a 1° by 1° grid. In this case the observed CO columns above the clouded ocean scenes are filled up with modeled CO below the cloud to obtain a total column. It can be seen that there are no sharp discontinuities in the CO total columns between land and ocean scenes, indicating that filling up the observed CO partial columns with modeled CO below the cloud is a useful tool to obtain CO total columns over ocean scenes. The five year average shows the same global patterns over the oceans as seen in the annual means in Fig. 10. Over land the well-known biomass burning emission regions in equatorial Africa and South America are clearly visible (Fig. 11), as are the emission regions in South and Southeastern Asia in both observed and modeled CO. Especially over Asia and at mid- and high-northern latitudes CO tends to be higher than the model values. This is probably due to too low emissions in the TM4 model especially

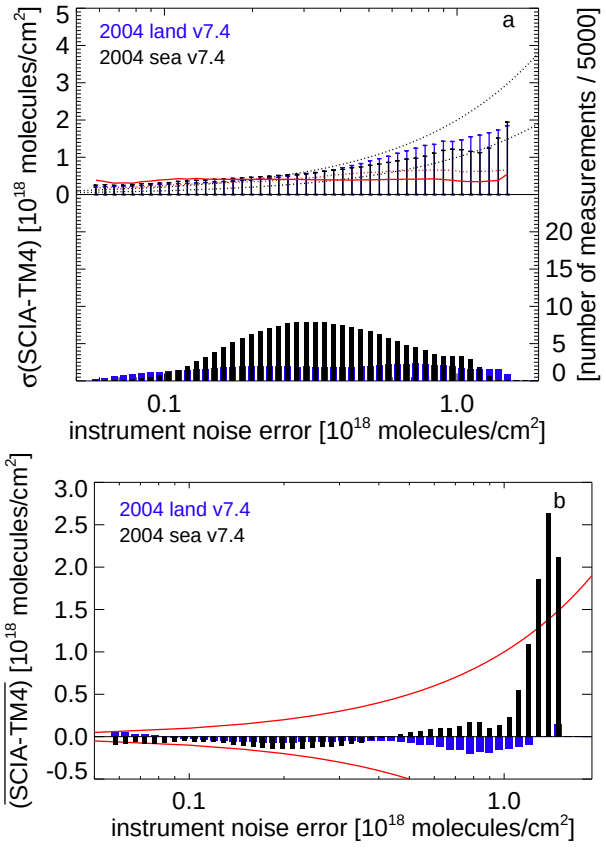

Fig. 8. Comparison of the single SCIAMACHY CO total column measurements over land and partial CO total columns over clouded ocean scenes for the period January to December 2004. **(a)** Root mean square (rms) values of the differences between the single SCIAMACHY CO measurements and the spatially and temporally collocated TM4 CO columns as function of the instrument-noise error. The blue bars indicate the distribution based on the observations over land, the black bars are based on the clouded ocean observations. The black dotted lines indicate the 1- and 2-σ instrument-noise error levels. The red lines indicate the rms value of the TM4 simulated CO total columns over land (dotted line) and over clouded ocean scenes (solid line). The blue (land) and black (clouded ocean scenes) bars in the bottom panel denote the number of measurements for each instrument-noise interval. **(b)** Average differences between the single SCIAMACHY CO measurements and the spatially and temporally collocated TM4 CO columns as function of the instrument-noise error. The bars indicate the mean difference for each instrument-noise interval. The blue bars indicate land observations, the black bars clouded ocean observations. The red line indicates the 1-σ instrument-noise error levels.

over Asia which is also seen in other models which use similar or different emission inventories and indicated by inverse modeling studies (Shindell et al., 2006; Turquety et al., 2008; Tanimoto et al., 2008; Kopacz et al., 2009).

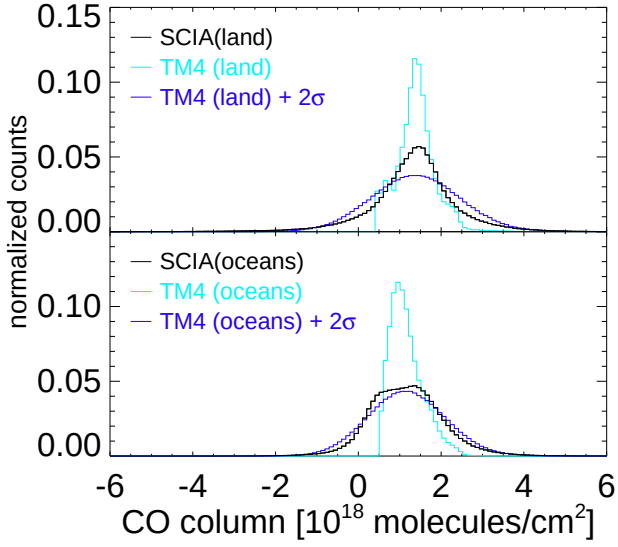

Fig. 9. Normalized probability distribution of SCIAMACHY CO columns based on daily gridded $1° \times 1°$ observations for 2004. Only SCIAMACHY CO measurements with random instrument-noise errors $<1.5 \times 10^{18}$ molecules/cm^2 have been taken into account. The black lines indicate the SCIAMACHY CO column distribution, the light blue lines the corresponding TM4 CO column distributions, while the blue lines denote the TM4 distribution convoluted with artificial Gaussian noise corresponding to $2\times$ the mean instrument-noise error. Top panel: SCIAMACHY CO total column measurements over land with cloud fraction <0.2. Bottom panel: SCIAMACHY CO columns over the oceans above low clouds, i.e. with cloud top height >800 hPa and cloud fraction >0.2 together with the corresponding TM4 CO columns. Note that most CO emissions occur over land, while over the oceans only the partial column above the cloud is shown, compared to the total column over land. Both effects result in smaller observed columns over oceans compared to land.

Comparison of the CO total columns over the oceans in Fig. 11 with the partial columns above the clouds in Fig. 10 shows that the part below the clouds constitutes only a small fraction of the total column. Thus the CO columns over clouded ocean scenes represent the greater part of the actual total column over the oceans, typically ~60–80% with an average of approximately 75%.

4 Interannual variability

The availability of five years of CO column measurements allows for investigating interannual variability between 2003 and 2007 and possible global changes in the CO concentrations. Below we describe three regions with notable interannual variability in the CO columns.

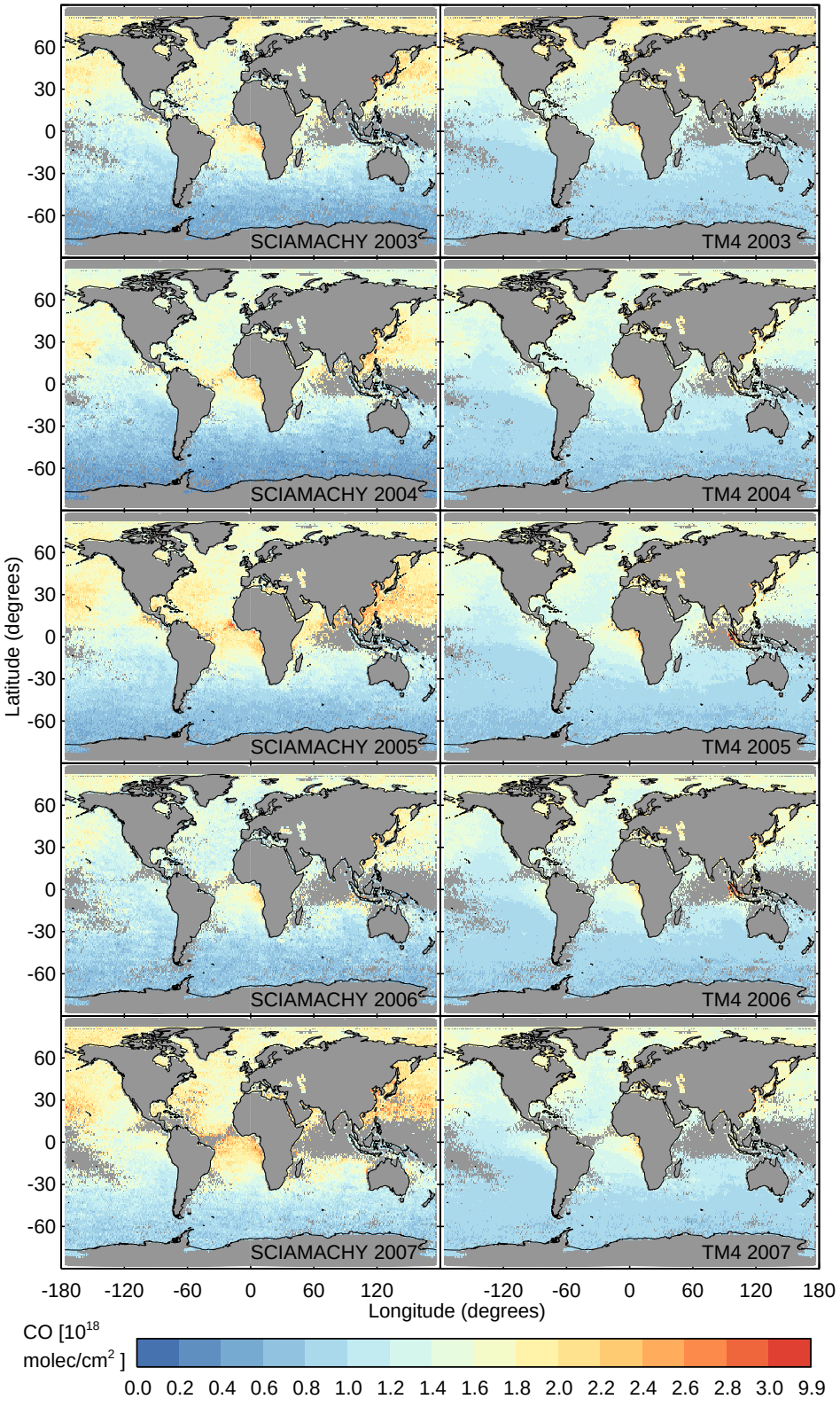

Fig. 10. Annual means of SCIAMACHY CO and TM4 CO columns above low clouds over the ocean on a 1° by 1° grid for the years 2003–2007. Blue indicates low CO columns and red high CO columns. Only grid boxes with more than 10 SCIAMACHY measurements per year are included.

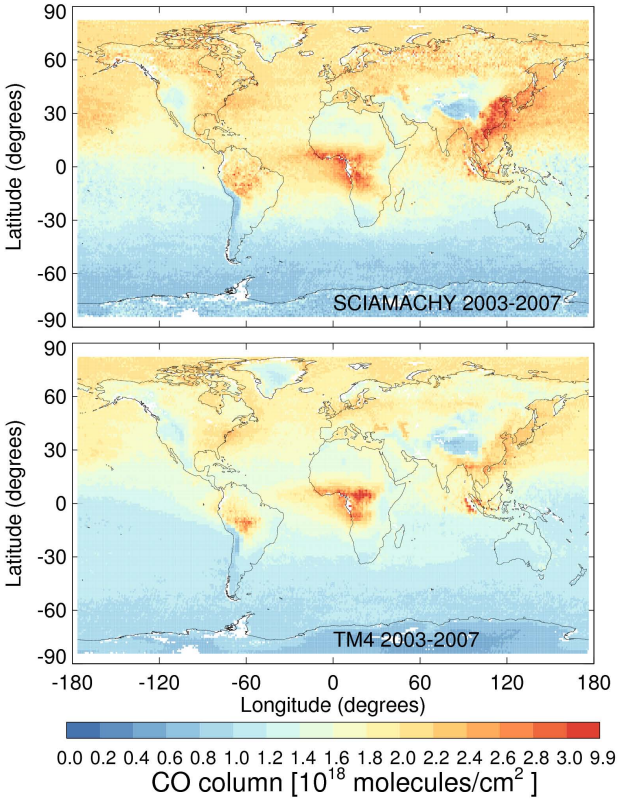

Fig. 11. Five year average CO total columns on a 1° by 1° grid. Top: SCIAMACHY CO. Bottom: TM4. Blue indicates low CO columns and red high CO columns. Note that the SCIAMACHY CO columns above low clouds over sea are filled up with TM4 CO below the cloud to obtain total columns.

4.1 Asian outflow

Turquety et al. (2008) have compared SCIAMACHY and MOPITT CO measurements over Asia with the LMDz-INCA model for the period March–May 2005 and conclude that their inventory-based model emissions are too low. A similar conclusion is drawn in the previous section for the TM4 model and is a common feature in atmospheric chemistry transport models (Shindell et al., 2006). Figure 12 shows the time series of measured and modeled CO total columns for the period January 2003–December 2007 over the area East of China indicated by the blue box in the bottom panels. The bottom panels show the monthly mean CO total columns over Asia and the northern Pacific in March 2006 and March 2007. Over the northern Pacific (clouded) ocean scenes the modeled below-cloud partial column is added to observed partial CO columns above the cloud. In this case, the modeled below-cloud partial column may be too low, because of too low emissions in the TM4 model (Shindell et al., 2006). The largest outflows of CO from Asia are observed in 2005 and 2007 while the outflow in 2006 was smaller. Pollution from Asia has little seasonality according to the TM4 model. Rather, the seasonality in CO seen in the time series is caused by the seasonality of OH concentrations which shows a minimum during local winter. The rapid decline of CO during late spring coincides with the rapid increase of OH during this time of year. The interannual variability seen in CO, with peaks in 2005 and 2007 is probably caused by biomass burning from southern Asia (Turquety et al., 2008) which may be underestimated in the TM4 model. Remaining calibration errors in the CO measurements as discussed in Gloudemans et al. (2008) may have a small effect on the absolute values of the observed CO columns, but are unlikely to affect the observed variability. Annual differences in cloud cover and hence in the number of clouded ocean measurements have been accounted for by averaging over a variable time period in order to warrant sufficient precision of the observed CO columns and consequently the observed variability.

4.2 Indonesia

Figure 13 shows the time series of measured and modeled CO total columns for the period January 2003–December 2007 averaged over the area west of Indonesia indicated by the blue box in the bottom panels. This area is mainly affected by biomass burning originating in Indonesia. The bottom panels show the monthly mean CO total columns over Indonesia and the surrounding oceans for October and November 2006 when extensive biomass burning was taking place in Indonesia. The time series show that the CO columns in 2006 during the biomass-burning season are significantly higher than in other years. The interannual variability seen in SCIAMACHY CO for the period 2003–2007 corresponds well with that seen in the MOPITT CO data (http://www.nasa.gov/centers/goddard/news/topstory/2007/elnino_wildfire.html) although measured SCIAMACHY columns were substantially higher than those measured by MOPITT during the 2006 peak fire months. Both SCIAMACHY and MOPITT observed large CO columns during spring 2005 and autumn 2006 with the largest peak in 2006, and much lower CO columns during the rest of both years as well as in 2003, 2004 and 2007. Comparison with the ESPI ENSO Index suggests that peaks in CO over Indonesia in the period 2003–2007 coincide with the warm phases of El Niño which led to an extended dry season and an increase in the biomass-burning over Indonesia. In October/November 2007 the SCIAMACHY CO columns are similar to those in 2005 and consistent with the monthly MOPITT CO images (http://web.eos.ucar.edu/mopitt/data/plots/mapsv3_mon.html) indicating that less biomass burning occurred in Indonesia during autumn 2007 and 2005 compared to autumn 2006 and 2004.

The recurring small annual peak in CO in late winter and early spring in the period January–March in this region coincides with the seasonality of transported pollution from the

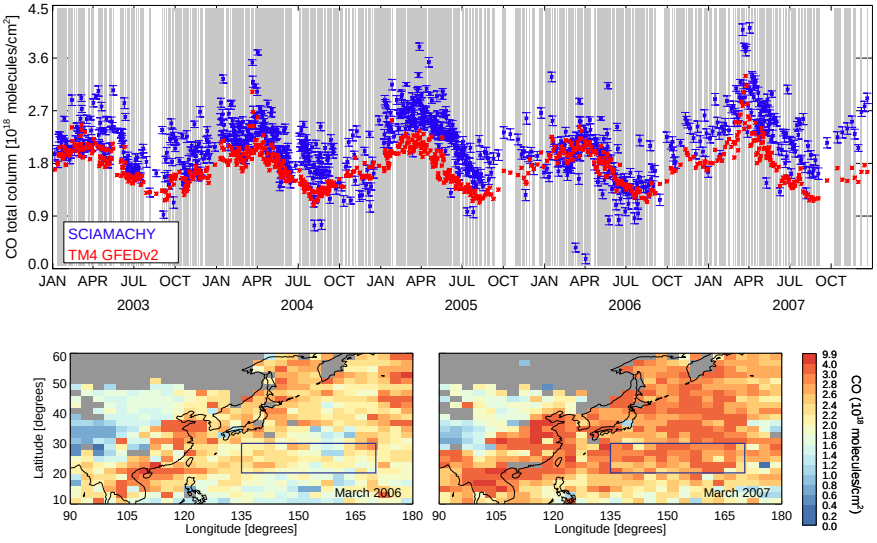

Fig. 12. Top panel: timeseries for the period January 2003–December 2007 using SCIAMACHY CO measurements averaged over the area East of China as indicated by the blue boxes in the bottom panels. The SCIAMACHY CO measurements are averaged over a varying time period indicated by the grey vertical bars in order to obtain an instrument-noise error of 1×10^{17} molecules/cm^2 for each SCIAMACHY data point (blue). The red stars indicate the spatially and temporally collocated TM4 CO total columns. The SCIAMACHY CO columns above the clouded ocean scenes are filled with the TM4 CO column below clouds to obtain a total column. Year-to-year variations are clearly seen. Bottom left panel: Asian outflow in March 2006. Monthly mean $3°\times2°$ SCIAMACHY CO total columns. Over sea the columns below the clouds are filled with TM4 values. Blue indicates low CO columns and red high CO columns. Bottom right panel: as bottom left panel, but for March 2007.

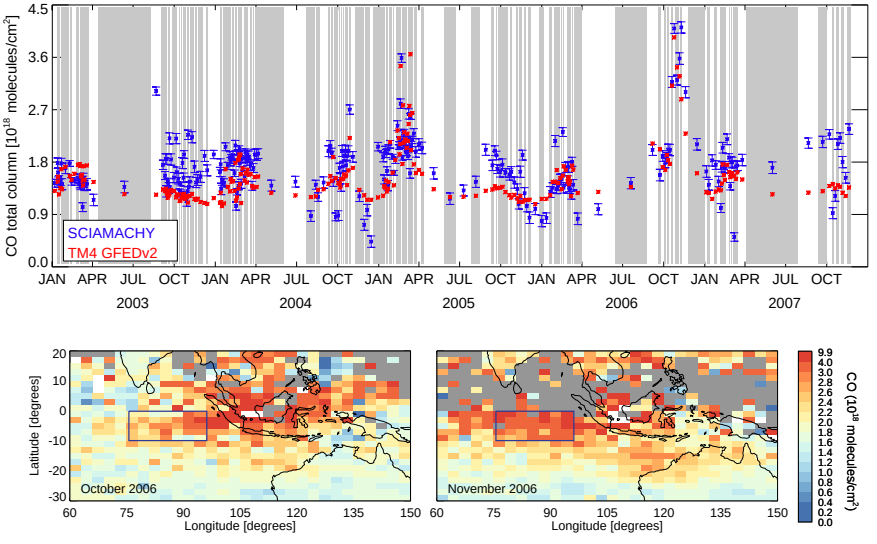

Fig. 13. Top panel: timeseries for the period January 2003–December 2007 using SCIAMACHY CO measurements averaged over the area West of Indonesia as indicated by the blue boxes in the bottom panels. The SCIAMACHY CO measurements are averaged over a varying time period indicated by the grey vertical bars in order to obtain an instrument-noise error of 1×10^{17} molecules/cm^2 for each SCIAMACHY data point (blue). The red stars indicate the spatially and temporally collocated TM4 CO total columns. The SCIAMACHY CO columns above the clouded ocean scenes are filled with the TM4 CO column below clouds to obtain a total column. Note that in October/November 2006 CO columns are significantly higher than in other years. Bottom left panel: Indonesia in October 2006. Monthly mean $3°\times2°$ SCIAMACHY CO total columns. Over sea the columns below the clouds are filled with TM4 values. Blue indicates low CO columns and red high CO columns. Bottom right panel: as bottom left panel, but for November 2006.

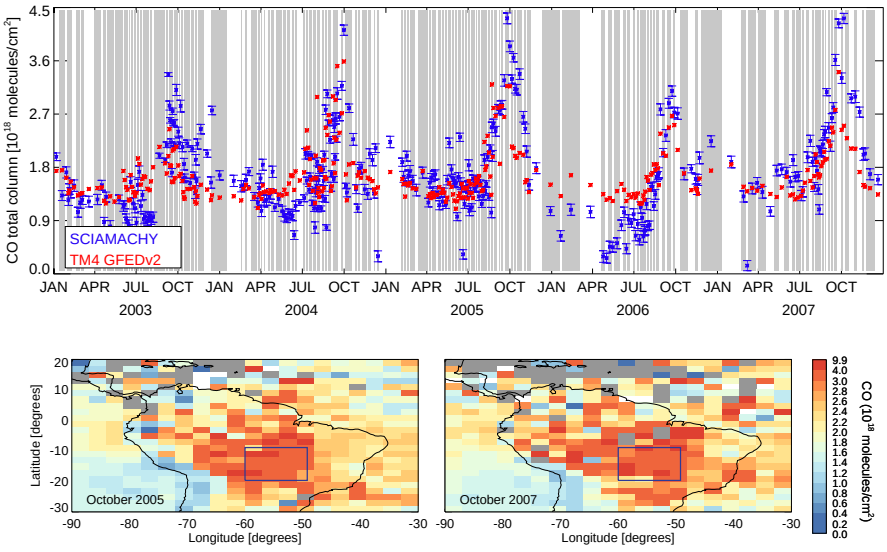

Fig. 14. Top panel: timeseries for the period January 2003–December 2007 over Brazil using SCIAMACHY CO measurements averaged over the area indicated by the blue boxes in the bottom panels. The SCIAMACHY CO measurements are averaged over a varying time period indicated by the grey vertical bars in order to obtain an instrument-noise error of 1×10^{17} molecules/cm^2 for each SCIAMACHY data point (blue). The red stars indicate the spatially and temporally collocated TM4 CO total columns. Note that in October 2004, 2005, and 2007 the CO total columns are significantly higher than in October 2003 and 2006. Bottom left panel: Brazil in October 2005. Monthly mean $3°\times2°$ SCIAMACHY CO total columns. Over sea the columns below the clouds are filled with TM4 values. Over land SCIAMACHY CO total columns are shown (cf. Sect. 3). Blue indicates low CO columns and red high CO columns. Bottom right panel: as bottom left panel, but for October 2007.

Indian continent which affects most of the Indian Ocean atmosphere north of the ITCZ (Lelieveld et al., 2001; de Laat et al., 2001), and is otherwise known as the Asian Brown Cloud (Ramanathan et al., 2007; Seinfeld, 2008).

4.3 Amazonia

Figure 14 shows the time series of observed and modeled CO total columns for the period January 2003–December 2007 over an active deforestation region in Amazonia outlined by the blue box in the bottom panels. The panels show the monthly mean CO total columns in October for the years 2005 and 2007. The CO columns for October, the peak of the biomass burning season, for 2004, 2005, and 2007 are significantly higher than in October 2003 and 2006, highlighting the large interannual variability of CO and biomass burning in this region. This is in good agreement with the variation in the annual GFEDv2 emissions here, which are 23.3, 42.4, 42.4, 16.9, and 56.8 Tg CO yr^{-1} for 2003, 2004, 2005, 2006, and 2007, respectively. A similar variability in the GFEDv2 emissions is seen over South America as a whole. The interannual variation in the CO columns is mostly influenced by biomass burning in Amazonia which takes place during the August-November period and is partly related to precipitation rates during the dry season (van der Werf et al., 2008) and socio-economic factors (Morton et al., 2006). The dry season in 2006 was relatively wet (cf. http://precip.gsfc.nasa.gov/rain_pages/rainrate_monthly_version2.html) and observations confirm that biomass burning emissions were relatively low in 2006. In contrast, CO columns in 2007 indicate that biomass burning emissions have increased again, suggesting that the low emissions in 2006 were more likely related to unfavorable climate conditions than the political incentives taken to reduce fire and deforestation (Koren et al., 2007). A similar interannual variation is seen in the monthly MOPITT CO images (http://web.eos.ucar.edu/mopitt/data/plots/mapsv3_mon.html). In addition, Petersen et al. (2008) have observed similar interannual changes in both the FTIR measurements and MOPITT data over Paramaribo for the years 2004, 2005, and 2006. In a future study we aim to use SCIAMACHY measurements to provide a more quantitative perspective on emissions.

5 Conclusions

This paper presents a new version of the IMLM method for the retrieval of SCIAMACHY CO columns from the 2.3 μm wavelength range. The new version includes a more accurate determination of the random instrument-noise error for CO which leads to smaller rms differences between single CO measurements and the corresponding model values. The new version also uses updated spectroscopic parameters for H_2O and CH_4 but this has only a minor impact on the retrieved

CO columns. The data set has been extended to five years of CO column observations covering the period 2003 to 2007. In addition, CO measurements over partially clouded ocean scenes are included which increases the number of useful CO measurements by almost a factor of 4. The CO measurements over clouded ocean scenes have been compared with the collocated modeled CO columns over the same clouds and compare well. In order to do this the CH_4 columns retrieved simultaneously with the CO columns are used to determine the cloud top height. The CH_4 cloud top height is in good agreement with the FRESCO+ cloud top height determined from the SCIAMACHY oxygen-A band measurements and thus indicates that the CH_4 cloud top height is a good diagnostic of the cloud top height over clouded ocean scenes. Significant interannual variability is seen in CO over the period 2003–2007. Three examples are highlighted: the Asian outflow of pollution over the northern Pacific, the biomass-burning outflow over the Indian Ocean originating from Indonesia, and biomass burning in Amazonia. In general there is a very good agreement between observed and modeled seasonal cycles and interannual variability. The new data set covering five years of SCIAMACHY data over land and sea thus provides useful information for investigating interannual variability and will help to further constrain emission sources of CO on a global scale, e.g. using inverse modeling techniques.

Acknowledgements. SCIAMACHY is a joint project of the German Space Agency DLR and the Dutch Space Agency NIVR with contribution of the Belgian Space Agency. We thank the Netherlands SCIAMACHY Data Center and ESA for providing data. The work performed is (partly) financed by NIVR. The authors thank Piet Stammes for useful discussions on the FRESCO+ algorithm and for providing the FRESCO+ data, and Christian Frankenberg for useful discussions on the spectroscopy.

Edited by: W. Lahoz

References

Bovensmann, H., Burrows, J. P., Buchwitz, M., Frerick, J., Noël, S., Rozanov, V. V., Chance, K. V., and Goede, A.: SCIAMACHY: Mission Objectives and Measurement Modes, J. Atmos. Sci., 56, 127–150, 1999.

Bowman, K. P.: Transport of carbon monoxide from the tropics to the extratropics, J. Geophys. Res., 111, D02107, doi:10.1029/2005JD006137, 2006.

Buchwitz, M., de Beek, R., Noël, S., Burrows, J. P., Bovensmann, H., Schneising, O., Khlystova, I., Bruns, M., Bremer, H., Bergamaschi, P., Körner, S., and Heimann, M.: Atmospheric carbon gases retrieved from SCIAMACHY by WFM-DOAS: version 0.5 CO and CH4 and impact of calibration improvements on CO_2 retrieval, Atmos. Chem. Phys., 6, 2727–2751, 2006, http://www.atmos-chem-phys.net/6/2727/2006/.

Buchwitz, M., Khlystova, I., Bovensmann, H., and Burrows, J. P.: Three years of global carbon monoxide from SCIAMACHY: comparison with MOPITT and first results related to the detection of enhanced CO over cities, Atmos. Chem. Phys., 7, 2399–2411, 2007, http://www.atmos-chem-phys.net/7/2399/2007/.

Cicerone, R. J.: How has the Atmospheric Concentration of CO changed, in: The Changing Atmosphere, edited by: Rowland, F. S. and Isaksen, I. S. A., Wiley, 49–61, 1988.

Deeter, M. N., Emmons, L. K., Francis, G. L., et al.: Operational carbon monoxide retrieval algorithm and selected results for the MOPITT instrument, J. Geophys. Res., 108(D14), 4399, doi:10.1029/2002JD003186, 2003.

De Laat, A. T. J., Lelieveld, J., Dickerson, R. R., Lobert, J., and Roelofs, G. J.: Source analysis of carbon monoxide pollution during INDOEX 1999, J. Geophys. Res., 106, 28481–28495, 2001.

De Laat, A. T. J., Gloudemans, A. M. S., Schrijver, H., van den Broek, M. M. P., Meirink, J. F., Aben, I., and Krol, M.: Quantitative analysis of SCIAMACHY carbon monoxide total column measurements, Geophys. Res. Lett., 33, L07807, doi:10.1029/2005GL025530, 2006.

De Laat, A. T. J., Gloudemans, A. M. S., Aben, I., Krol, M., Meirink, J. F., van der Werf, G. R., and Schrijver, H.: SCIAMACHY carbon monoxide total columns: statistical evaluation and comparison with CTM results, J. Geophys. Res., 112, D12310, doi:10.1029/2006JD008256, 2007.

Edwards D. P., Emmons, L. K., Hauglustaine, D. A., et al.: Observations of carbon monoxide and aerosols from the Terra satellite: Northern Hemisphere variability, J. Geophys. Res., 109, D24202, doi:10.1029/2004JD004727, 2004.

Edwards, D. P., Emmons, L. K., Gille, J. C., et al.: Satellite-observed pollution from Southern Hemisphere biomass burning, J. Geophys. Res., 111, D14312, doi:10.1029/2005JD006655, 2006a.

Edwards D. P., Pétron, G., Novelli, P. C., Emmons, L. K., Gille, J. C., and Drummond, J. R.: Southern Hemisphere carbon monoxide interannual variability observed by Terra/Measurement of Pollution in the Troposphere (MOPITT), J. Geophys. Res., 111, D16303, doi:10.1029/2006JD007079, 2006b.

Frankenberg, C., Platt, U., and Wagner, T.: Retrieval of CO from SCIAMACHY onboard ENVISAT: detection of strongly polluted areas and seasonal patterns in global CO abundances, Atmos. Chem. Phys., 5, 1639–1644, 2005, http://www.atmos-chem-phys.net/5/1639/2005/.

Giglio, L., van der Werf, G. R., Randerson, J. T., Collatz, G. J., and Kasibhatla, P.: Global estimation of burned area using MODIS active fire observations, Atmos. Chem. Phys., 6, 957–974, 2006, http://www.atmos-chem-phys.net/6/957/2006/.

Gloudemans, A. M. S., Schrijver, H., Kleipool, Q., van den Broek, M. M. P., Straume, A. G., Lichtenberg, G., van Hees, R. M., Aben, I., and Meirink, J. F.: The impact of SCIAMACHY near-infrared instrument calibration on CH_4 and CO total columns, Atmos. Chem. Phys., 5, 2369–2383, 2005, http://www.atmos-chem-phys.net/5/2369/2005/.

Gloudemans, A. M. S., Krol, M. C., Meirink, J. F., de Laat, A. T. J., van der Werf, G. R., Schrijver, H., van den Broek, M. M. P., and Aben, I.: Evidence for long-range transport of Carbon Monoxide in the Southern Hemisphere from SCIAMACHY observations, Geophys. Res. Lett., 33, L16807, doi:10.1029/2006GL026804, 2006.

Gloudemans, A. M. S., Schrijver, H., Hasekamp, O. P., and Aben, I.: Error analysis for CO and CH_4 total column retrievals from SCIAMACHY 2.3 μm spectra, Atmos. Chem. Phys., 8, 3999–4017, 2008, http://www.atmos-chem-phys.net/8/3999/2008/.

Heald, C. L., Jacob, D. J., Jones, D. B. A., Palmer, P. I., Logan, J. A., Streets, D. G., Sachse, G. W., Gille, J. C., Hoffman, R. N., and Nehrkorn, T.: Comparative inverse analysis of satellite (MOPITT) and aircraft (TRACE-P) observations to estimate Asian sources of carbon monoxide, J. Geophys. Res., 109, D23306, doi:10.1029/2004JD005185, 2004.

Jenouvrier, A., Daumonta, L., Régalia-Jarlot, L., Tyuterev, V. G., Carleer, M., Vandaele, A. C., Mikhailenko, S., and Fally, S.: Fourier transform measurements of water vapor line parameters in the 4200–6600 cm^{-1} region, J. Quant. Spectrosc. Ra., 105, 326–355, 2007.

Kopacz, M., Jacob, D. J., Henze, D. K., Heald, C. L., Streets, D. G., and Zhang, Q.: Comparison of adjoint and analytical Bayesian inversion methods for constraining Asian sources of carbon monoxide using satellite (MOPITT) measurements of CO columns, J. Geophys. Res., 114, D04305, doi:10.1029/2007JD009264, 2009.

Koren, I., Remer, L. A., and Longo, K.: Reversal of trend of biomass burning in the Amazon, Geophys. Res. Lett., 34, L20404, doi:10.1029/2007GL031530, 2007.

Krijger, J. M., Aben, I., and Schrijver, H.: Distinction between clouds and ice/snow covered surfaces in the identification of cloud-free observations using SCIAMACHY PMDs, Atmos. Chem. Phys., 5, 2729–2738, 2005, http://www.atmos-chem-phys.net/5/2729/2005/.

Lelieveld, J., Crutzen, P. J., Ramanathan, V., et al.: The Indian Ocean Experiment: Widespread air pollution from south and southeast Asia, Science, 291, 1031–1036, 2001.

McMillan, W. W., Barnet, C., Strow, L., et al.: Daily global maps of carbon monoxide from NASA's Atmospheric Infrared Sounder, Geophys. Res. Lett., 32, L11801, doi:10.1029/2004GL021821, 2005.

Meirink, J. F., Eskes, H. J., and Goede, A. P. H.: Sensitivity analysis of methane emissions derived from SCIAMACHY observations through inverse modelling, Atmos. Chem. Phys., 6, 1275–1292, 2006, http://www.atmos-chem-phys.net/6/1275/2006/.

Morton, D. C., DeFries, R. S., Shimabukuro, Y. E., Anderson, L. O., Arai, E., Espirito-Santo, F. D., Freitas, R., and Morisette, J.: Cropland expansion changes deforestation dynamics in the southern Brazilian Amazon, Proceedings of the National Academy of Sciences of the United States of America, 103(39), 14637–14641, doi:10.1073/pnas.0606377103, 2006.

Petersen A. K., Warneke, T., Lawrence, M. G., Notholt, J., and Schrems, O.: First ground-based FTIR observations of the seasonal variation of carbon monoxide in the tropics, Geophys. Res. Lett., 35, L03813, doi:10.1029/2007GL031393, 2008.

Predoi-Cross, A., Brawley-Tremblay, M., Brown, L. R., Malathy Devi, V., and Chris Benner, D.: Multispectrum analysis of $^{12}CH_4$ from 4100 to 4635 cm^{-1}: II. Air-broadening coefficients (widths and shifts), J. Mol. Spectrosc. 236, 201–215, 2006.

Ramanathan, V., Ramana, M. V., Roberts, G., Kim, D., Corrigan, C., Chung, C., and Winker, D.: Warming trends in Asia amplified by brown cloud solar absorption, Nature, 448, 575–578, doi:10.1038/nature06019, 2007.

Rothman, L. S., Jacquemart, D., Barbe, A., et al.: The HITRAN 2004 molecular spectroscopic database, J. Quant. Spectrosc. Ra., 96, 139–204, 2005.

Schrijver, H.: Retrieval of carbon monoxide, methane and nitrous oxide from SCIAMACHY measurements, in Proc. ESAMS, European Symposium on Atmospheric Measurements from Space, ESA WPP-161 1, ESTEC, Noordwijk, The Netherlands, 285–294, 1999.

Seinfeld, J.: Black carbon and brown clouds, Nature Geosci., 1, 15–16, doi:10.1038/ngeo.2007.62, 2008.

Shindell, D. T., Faluvegi, G., Stevenson, D. S., et al.: Multimodel simulations of carbon monoxide: Comparison with observations and projected near-future changes, J. Geophys. Res., 111, D19306, doi:10.1029/2006JD007100, 2006.

Stohl, A., Eckhardt, S., Forster, C., James, P., and Spichtinger, N.: On the pathways and timescales of intercontinental air pollution transport, J. Geophys. Res., 107(D23), 4684, doi:10.1029/2001JD001396, 2002.

Tanimoto, H., Sawa, Y., Yonemura, S., Yumimoto, K., Matsueda, H., Uno, I., Hayasaka, T., Mukai, H., Tohjima, Y., Tsuboi, K., and Zhang, L.: Diagnosing recent CO emissions and ozone evolution in East Asia using coordinated surface observations, adjoint inverse modeling, and MOPITT satellite data, Atmos. Chem. Phys., 8, 3867–3880, 2008, http://www.atmos-chem-phys.net/8/3867/2008/.

Turquety, S., Clerbaux, C., Law, K., Coheur, P.-F., Cozic, A., Szopa, S., Hauglustaine, D. A., Hadji-Lazaro, J., Gloudemans, A. M. S., Schrijver, H., Boone, C. D., Bernath, P. F., and Edwards, D. P.: CO emission and export from Asia: an analysis combining complementary satellite measurements (MOPITT, SCIAMACHY and ACE-FTS) with global modeling, Atmos. Chem. Phys., 8, 5187–5204, 2008, http://www.atmos-chem-phys.net/8/5187/2008/.

van der Werf, G. R., Randerson, J. T., Giglio, L., Collatz, G. J., Kasibhatla, P. S., and Arellano Jr., A. F.: Interannual variability in global biomass burning emissions from 1997 to 2004, Atmos. Chem. Phys., 6, 3423–3441, 2006, http://www.atmos-chem-phys.net/6/3423/2006/.

van der Werf, G. R., Randerson, J. T., Giglio, L., Gobron, N., and Dolman, A. J.: Climate controls on the variability of fires in the tropics and subtropics, Global Biogeochemical Cycles, Global Biogeochem. Cy., 22, GB3028, doi:10.1029/2007GB003122, 2008.

Wang, P., Stammes, P., van der A, R., Pinardi, G., and van Roozendael, M.: FRESCO+: an improved O_2 A-band cloud retrieval algorithm for tropospheric trace gas retrievals, Atmos. Chem. Phys., 8, 6565–6576, 2008, http://www.atmos-chem-phys.net/8/6565/2008/.

Yurganov, L. N., McMillan, W. W., Dzhola, A. V., Grechko, E. I., Jones, N. B., and van der Werf, G. R.: Global AIRS and MOPITT CO measurements: Validation, comparison, and links to biomass burning variations and carbon cycle, J. Geophys. Res., 113, D09301, doi:10.1029/2007JD009229, 2008.